Supplemental Table 1. Expression profiling data showing *HOXA9* co-regulated genes (top panel) and *MIR196B* co-regulated genes (bottom panel) in 56 primary human AML samples.

	r-value	p-value (correlation)
MIR196B	0.641695	$8.41E^{-09}$
HOXA2	0.639705	$9.67E^{-09}$
HOXA3	0.842318	$1.45E^{-18}$
HOXA4	0.844739	$9.26E^{-19}$
HOXA5	0.867057	$9.94E^{-21}$
HOXA7	0.900317	$1.92E^{-24}$
HOXA10	0.938739	$7.59E^{-31}$
HOXB5	0.597966	$1.44E^{-07}$
HOXB6	0.621459	$3.31E^{-08}$
PBX3	0.658786	$2.44E^{-09}$
MEIS1	0.747463	$8.53E^{-13}$
MIR196A	0.807072	$1.23E^{-07}$
HOXA3	0.526948	$6.50E^{-06}$
HOXA4	0.557511	$1.41E^{-06}$
HOXA5	0.575272	$5.37E^{-07}$
HOXA7	0.590379	$2.26E^{-07}$
HOXA9	0.641695	$8.41E^{-09}$
HOXA10	0.602004	$1.13E^{-07}$

Supplemental Table 2. Flow cytometric analysis of (A) hematopoietic populations and (B) peripheral blood analysis of wild type mice after *in vivo* antagomir therapy (*n*=3 mice per treatment).

(A) Stem cell and Progenitor Analysis

	GMP	CMP	MEP	LT-HSC	ST-HSC	MPP	LK	LSK	L-KloS+
CA21+CA196b	44.47±4.27	35.03±4.89	8.29±2.46	2.09±0.85	16.20±3.47	78.03±4.36	32.00±10.23	4.24±1.53	3.29±1.17
A21	47.23±1.54	36.07±1.17	7.09±1.76	2.07±0.53	16.13±2.01	77.33±2.77	42.63±4.98	6.26±0.84	4.54±0.49
A196b	51.37±2.96*	29.17±3.66	8.03±2.25	3.31±1.27	18.73±1.08	72.87±3.06	34.40±5.07	4.13±0.99	3.82±1.33
A21+A196b	47.70±4.88	34.07±2.95	7.49±0.90	2.52±0.62	17.33±0.92	75.50±2.11	33.73±7.86	4.67±0.87	3.61±0.47

(B) Peripheral Blood Analysis

Range	**(1.8-10.7)**	**(0.1-2.4)**	**(45.4-60.3)**	**(0.0-0.4)**
	WBC	**NE**	**MCV**	**MO**
CA21+CA196b	6.35±2.2	3.072±1.74	44±0.58	0.206±0.08
A21	7.01±0.76	2.81±0.79	45.72±0.71	0.274±0.06
A196b	6.6±3.6	3.066±2.13	45.38±0.41	0.226±0.07
A21+A196b	8.22±4.27	3.438±3.10	45.76±0.20	0.324±0.22

Supplemental Figure 1. Velu & Chaubey

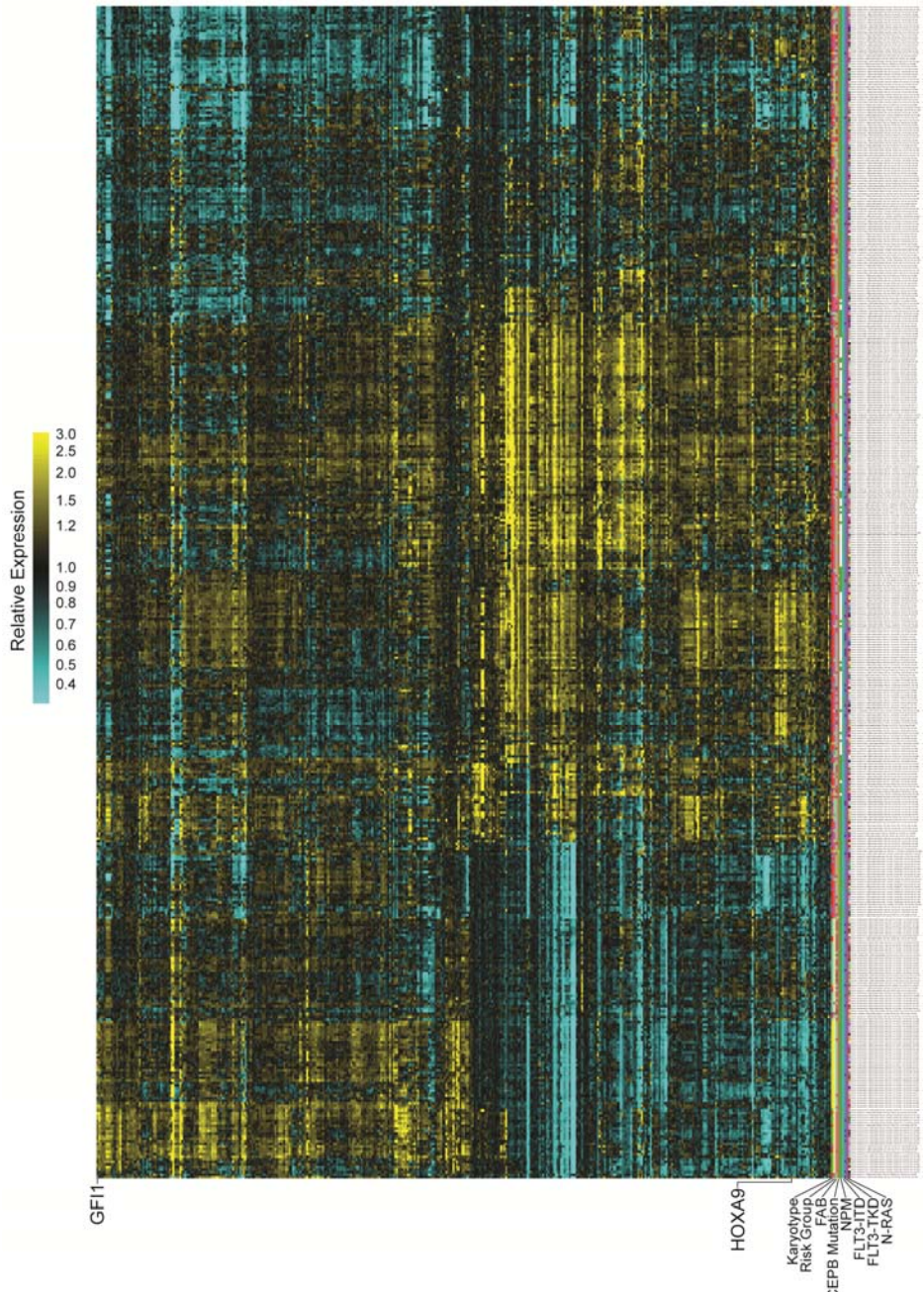

***NPM1*-mutant adult AML exhibit high *HOXA9*-like and low *GFI1*-like signatures.**

Hierarchical clustering of gene expression array data in 460 adult AML and MDS samples. The reciprocal relationship between *HOXA9*-like versus *GFI1*-like signatures is strongest in patients with either t(15;17), or t(8;21) translocations (*GFI1*-like) and in 11q23 or *NPM1*-mutant samples (*HOXA9*-like). MDS samples did not show an antagonistic relationship between GFI1 and HOXA9, possibly due to very low expression values of either gene.

Supplemental Figure 2. Velu & Chaubey

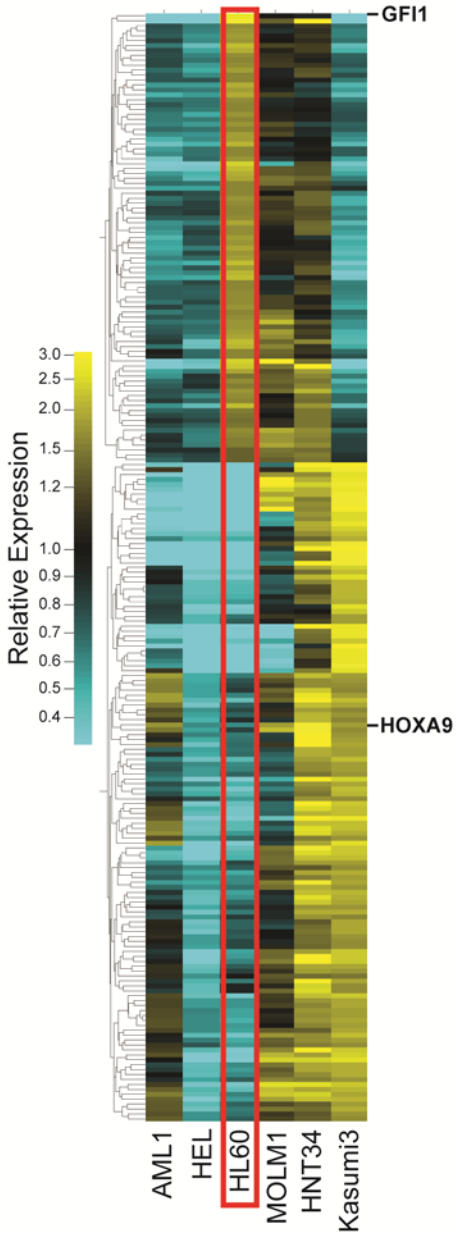

HL60 is a *GFI1*-like signature AML cell line. Hierarchical clustering of gene expression array data from human AML cell lines using the combined set of "*HOXA9*-like" and "*GFI1*-like" genes demonstrates a predominant *GFI1*-like signature in the HL60 cell line.

Supplemental Figure 3. Velu & Chaubey

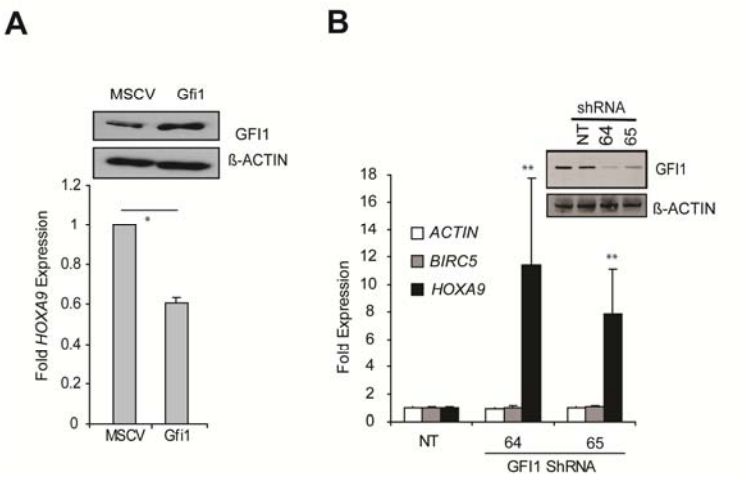

Gfi1 controls Hox expression. **(A)** TaqMan analysis of *HOXA9* in empty vector control (MSCV), and MSCV-Gfi1 transduced HL60 cells (*n*=3). Inset: immunoblot of GFI1 overexpression. **(B)** TaqMan analysis of *HOXA9* and two unrelated control genes (*ACTIN* and *BIRC5*) in HL60 cells transduced with *GFI1* shRNA-expressing lentiviruses (64 and 65) or a non-targeting control (NT) (*n*=3). Inset: immunoblot of GFI1 demonstrating knockdown. **P*<0.05, ***P*<0.01

Supplemental Figure 4. Velu & Chaubey

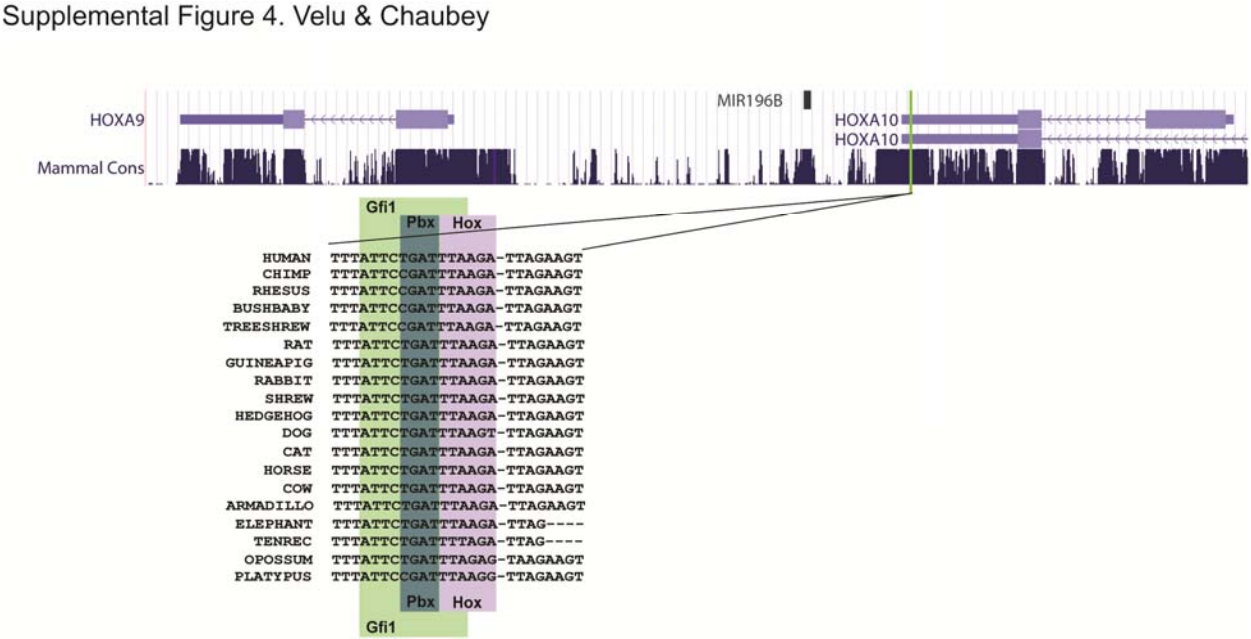

Gfi1-Hox binding site conservation. DNA sequence conservation of putative Gfi1-HoxA9-Pbx1-Meis1 binding site in the *Mir196b* promoter.

Supplemental Figure 5. Velu & Chaubey

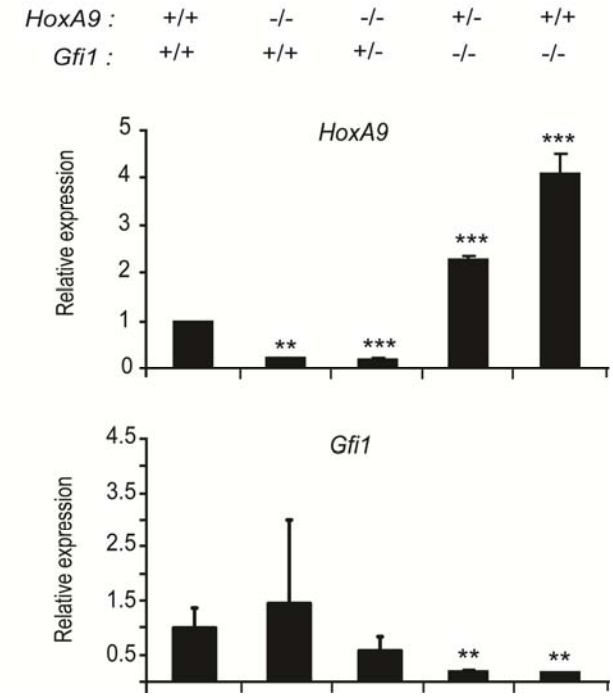

Validation of gene expression in mice with limiting alleles of Gfi1 or HoxA9. TaqMan analysis of *HoxA9* and *Gfi1* expression in Lin^- bone marrow cells from mice with limiting alleles of *HoxA9* and *Gfi1*. (*n*=3) ***P*<0.01, ****P*<0.001.

Supplemental Figure 6. Velu & Chaubey

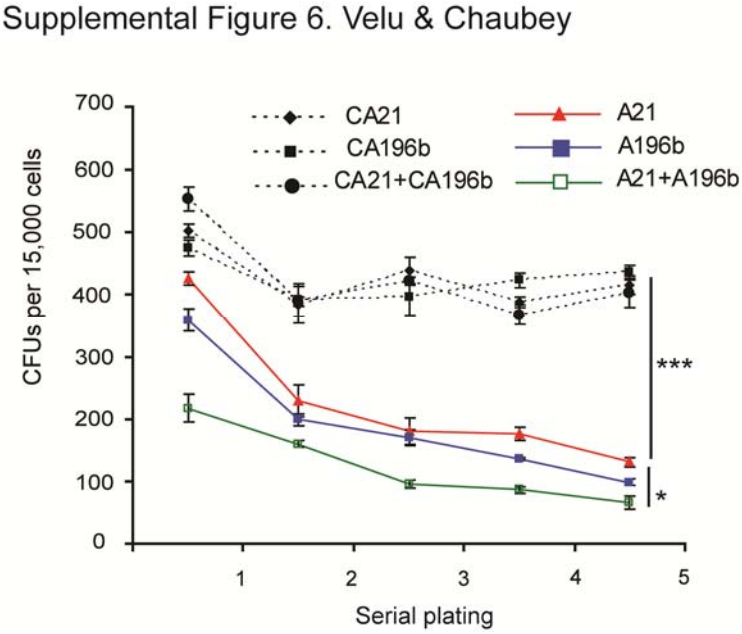

Antagomirs against miR-21 and miR-196b interfere with maintenance of MLL-oncoprotein-initiated leukemia. Enumeration of methylcellulose CFU with serial replating of an independent MLL-AF9 AML after antagomir treatment (*n*=3, mean±SD). ****P*<0.001

Supplemental Figure 7. Velu & Chaubey

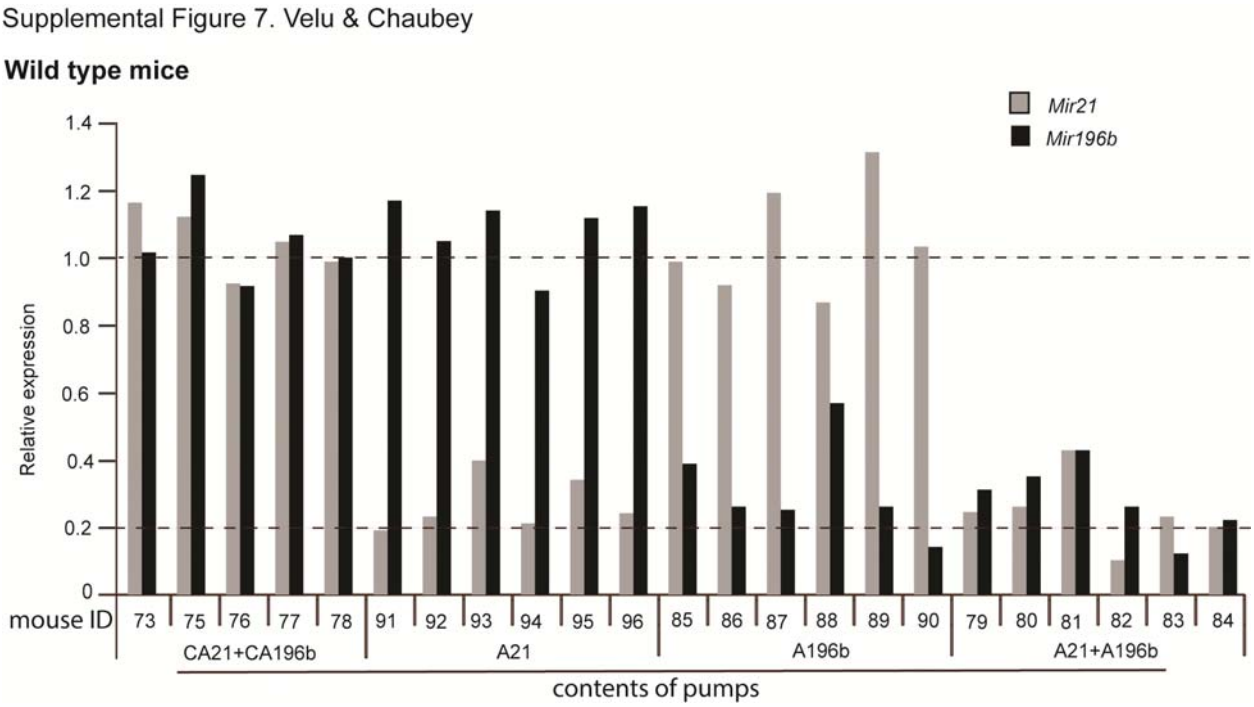

Efficacy of Antagomirs against miR-21 and miR-196b *in vivo*. TaqMan analysis of the steady state levels of mature miR-21 and miR-196b in the peripheral white blood cells of individual wild type mice seven days after implantation of pumps with the indicated antagomirs. Numbers denote individual mouse identifiers.

Supplemental Figure 8. Velu & Chaubey

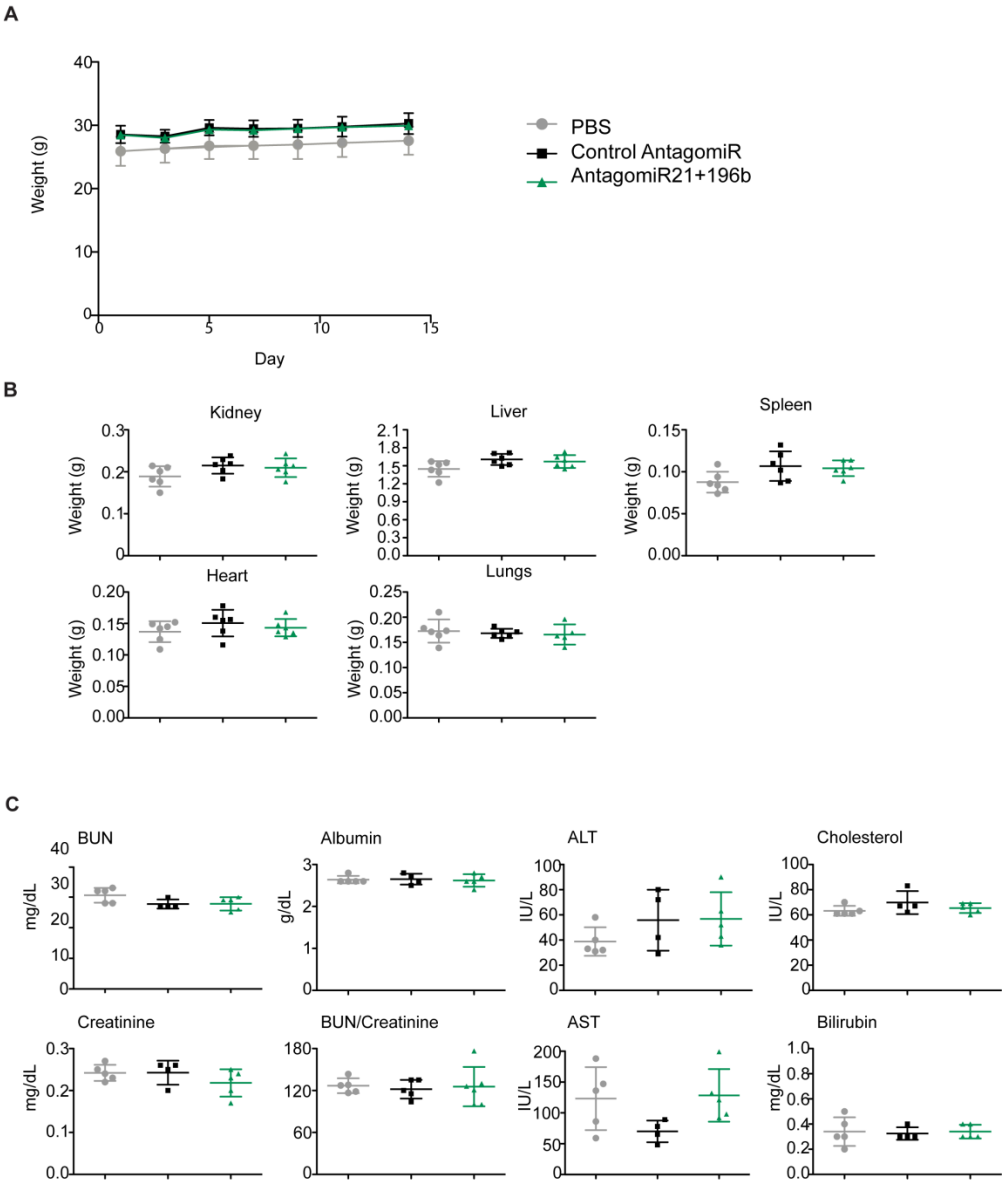

Toxicity assessment following the delivery of antagomiR21+196b in normal mice. (**A**) Total body weight, (**B**) weight of vital organs such as kidney, liver, spleen, heart and lungs, (**C**) blood chemistry such as levels of blood urea nitrogen (BUN), albumin, alanine aminotransferase (ALT), cholesterol, creatinine, BUN/Creatinine, aspartate aminotransferase (AST) and bilirubin were measured in normal mice after treatment with PBS, control antagomiR21+196b or antagomiR21+196b. Data are represented as mean±s.d (n=5 mice in each group). None of the groups show a statistically significant change.

Supplemental Figure 9. Velu & Chaubey

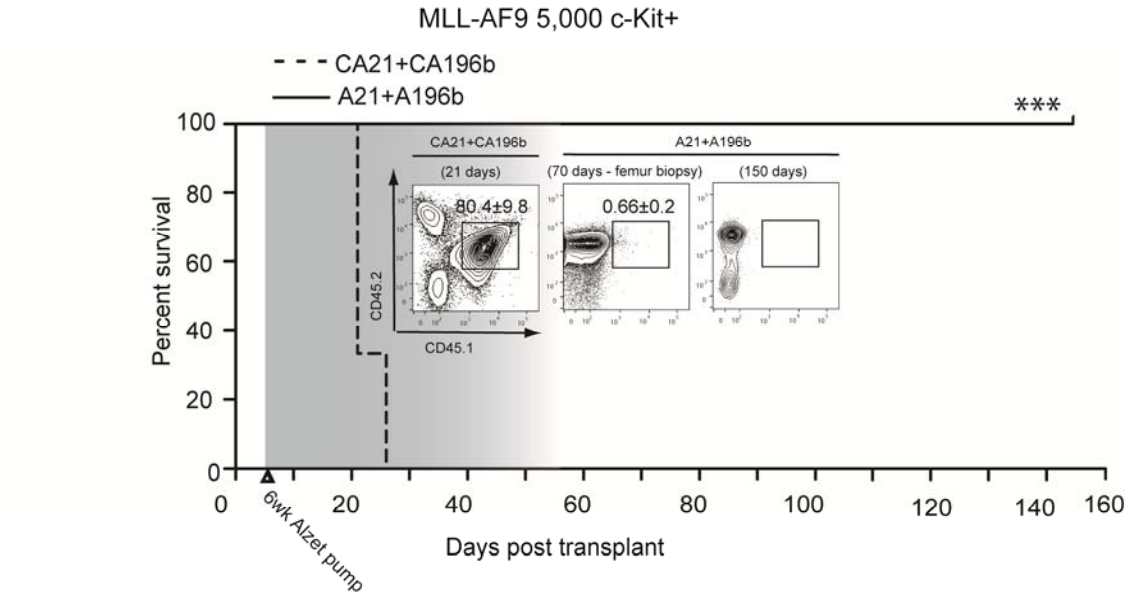

***In vivo* platform to test RNAi therapeutics by specifically interfering with miR-21 and miR-196b expression in MLL-AF9-initiated LIC.** Kaplan-Meier survival curve of partially conditioned C57Bl/6 mice (CD45.2$^+$) transplanted 5,000 c-Kit$^+$ CD45.1$^+$ CD45.2$^+$ MLL-AF9 leukemic splenocytes (*n*=4 recipient mice per group). Four days later, 6 week osmotic pumps containing A21+A196b or CA21+CA196b (shaded area denotes time of pump activity) were implanted in the mice and they were followed for survival. Insets show flow plots of MLL-AF9 c-Kit+ CD45.1+ CD45.2+ cells in mice at the indicated time points. ****P*<0.001.

Supplemental Figure 10. Velu & Chaubey

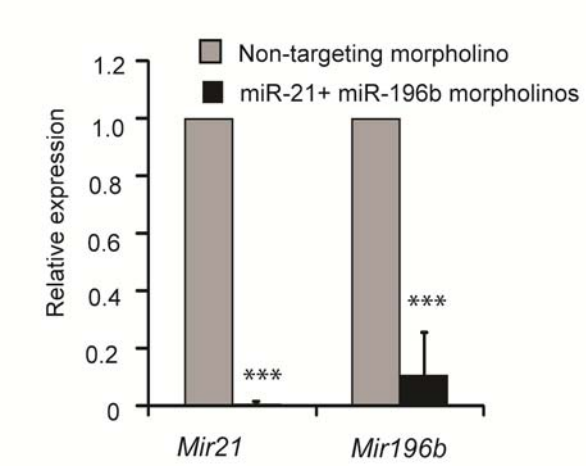

Quantitation of microRNA levels in c-Kit+ CD45.1+ CD45.2+ MLL-AF9-initiated leukemia cells treated with vivo-morpholino against miR-21 and miR-196b. TaqMan analysis of the steady state levels of mature miR-21 and miR-196b in c-Kit^{+} CD45.1^{+} CD45.2^{+} MLL-AF9 cells treated with either non-targeting (control) morpholino, or a combination of miR-21 and miR-196b morpholino for 72 hours (*n*=3, mean±SD). ****P*<0.001.

Supplemental Figure 11. Velu & Chaubey

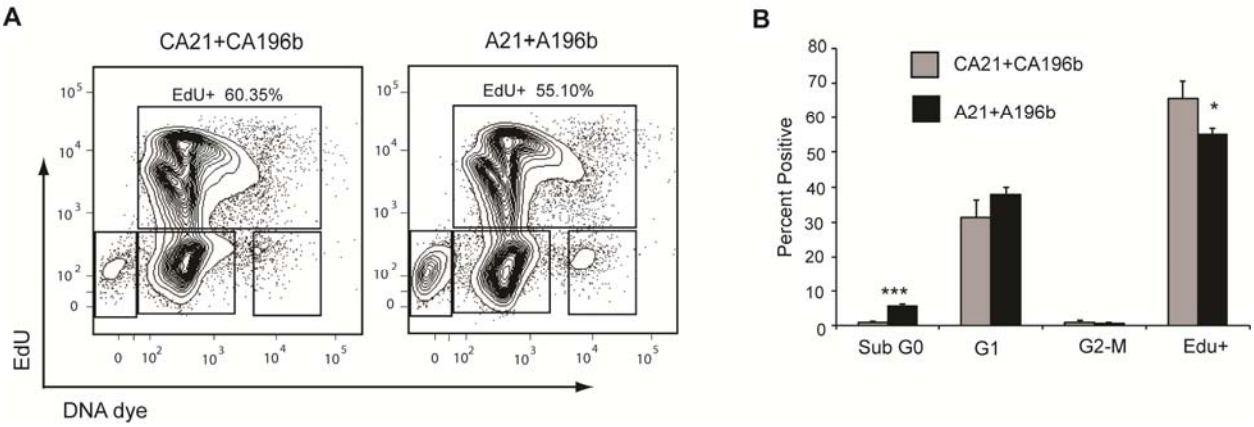

Antagomirs specifically block leukemia initiating stem cell activity in MLL-AF9-initiated leukemia. (A-B) Antagomir treatment modestly decreases proliferation of c-Kit$^+$ CD45.1$^+$ CD45.2$^+$ MLL-AF9 leukemia splenocytes (which are enriched for LIC). c-Kit$^+$ CD45.1$^+$ CD45.2$^+$ MLL-AF9 leukemic splenocytes were cultured with CA21+CA196b or A21+A196b for 72 hours in liquid culture with cytokines. Cells were then incubated with EdU for six hours, fixed, stained, analyzed by flow cytometry (**A**) and subpopulations were enumerated (**B**) (n=6). *P<0.05, ***P<0.001

Supplemental Figure 12. Velu & Chaubey

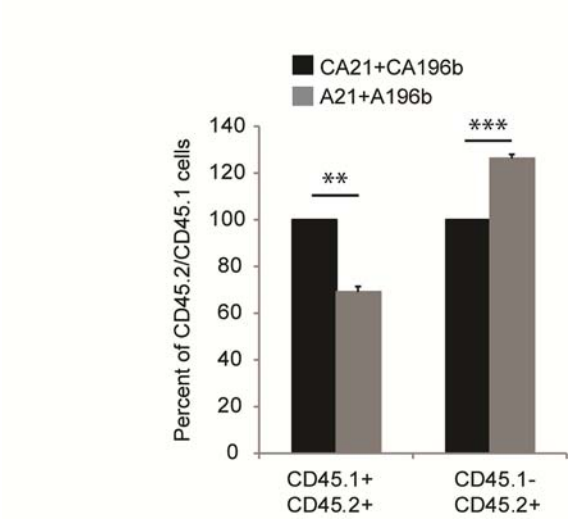

Antagomir treatment for 19 days *in vivo* decreases CD45.1+ CD45.2+ MLL-AF9-intiated leukemia cell burden. Sub-lethally irradiated mice were transplanted with c-Kit$^+$ CD45.1$^+$ CD45.2$^+$ MLL-AF9 leukemic splenocytes and the pumps were implanted at day 4 either with CA21+CA196b or A21+A196b. On day 19, mice were sacrificed, splenocytes isolated and analyzed by flow cytometry for leukemia (CD45.1+ CD45.2+) and recipient (CD45.2+) cells (*n*=3). Total absolute number of splenocytes (millions): control = 329.73 +/-5.90 versus antagomir = 320.13 +/-2.37. Total absolute number of CD45.1+CD45.2+ (MLL-AF9 leukemia) cells (millions): control = 151.28 +/-3.11 versus antagomir = 103.07 +/-4.65. ***P*<0.01, ****P*<0.001